CAMBRIDGE
UNIVERSITY PRESS

Article

Thermessaite-(NH₄), (NH₄)₂AlF₃(SO₄), a new fumarole mineral from La Fossa crater at Vulcano, Aeolian Islands, Italy

Anna Garavelli[1,2]* ⓘ, Daniela Pinto[1,2], Donatella Mitolo[3] and Uwe Kolitsch[4,5]

[1]Dipartimento di Scienze della Terra e Geoambientali, Università di Bari, via E. Orabona 4, I-70125 Bari, Italy; [2]Centro Interdipartimentale "Laboratorio di Ricerca per la Diagnostica dei Beni Culturali", Università di Bari, via E. Orabona 4, I-70125 Bari, Italy; [3]Autorità di Bacino Distrettuale dell'Appennino Meridionale Sede Puglia, Str. Prov. Per Casamassima km 3, I-70010 Valenzano (BA), Italy; [4]Mineralogisch-Petrographische Abt., Naturhistorisches Museum, Burgring 7, A-1010 Wien, Austria; and [5]Institut für Mineralogie und Kristallographie, Universität Wien, Althanstrasse 14, A-1090 Wien, Austria

Abstract

Thermessaite-(NH₄), ideally (NH₄)₂AlF₃(SO₄), is a new mineral found as a medium- to high-temperature (∼250–300°C) fumarole encrustation at the rim of La Fossa crater, Vulcano, Aeolian Islands, Italy. The mineral deposited as aggregates of minute (<0.2 mm) sharp prismatic crystals on the surface of a pyroclastic breccia in association with thermessaite, sulfur, arcanite, mascagnite, and intermediate members of the arcanite–mascagnite series.

The new mineral is colourless to white, transparent, non-fluorescent, has a vitreous lustre, and a white streak. The calculated density is 2.185 g/cm³. Thermessaite-(NH₄) is orthorhombic, space group *Pbcn*, with $a = 11.3005(3)$ Å, $b = 8.6125(3)$ Å, $c = 6.8501(2)$ Å, $V = 666.69(4)$ Å³ and $Z = 4$. The eight strongest reflections in the powder X-ray diffraction data [d in Å $(I)(hkl)$] are: 5.65 (100)(200), 4.84 (89)(111), 6.85 (74)(110), 3.06 (56)(112), 3.06 (53)(221), 3.08 (47)(311), 2.68 (28)(022) and 2.78 (26)(130). The average chemical composition, determined by quantitative SEM-EDS (N by difference), is (wt.%): K₂O 3.38, Al₂O₃ 25.35, SO₃ 36.58, F 26.12, (NH₄)₂O 22.47, O = F −11.00, total 102.90. The empirical chemical formula, calculated on the basis of 7 anions per formula unit, is $[(NH_4)_{1.85}K_{0.15}]_{\Sigma2.00}Al_{1.06}F_{2.94}S_{0.98}O_{3.06}$. The crystal structure, determined from single-crystal X-ray diffraction data [$R(F) = 0.0367$], is characterised by corner-sharing AlF₄O₂ octahedra which form [001] octahedral chains by sharing two *trans* fluoride atoms [Al–F2 = 1.8394(6) Å]. Non-bridging Al–F1 distances are shorter [1.756(1) Å]. The two *trans* oxygen atoms [Al–O = 1.920(2) Å] are from SO₄ tetrahedra. NH₄⁺ ions occur in layers parallel to (100) which alternate regularly with (100) layers containing ribbons of corner-sharing AlF₄O₂ octahedra and associated SO₄ groups. The NH₄⁺ ions are surrounded by five oxygen atoms and by four fluorine atoms. The mineral is named as the (NH₄)-analogue of thermessaite, K₂AlF₃(SO₄), and corresponds to an anthropogenic phase found in the burning Anna I coal dump of the Anna mine, Aachen, Germany. Both mineral and mineral name have been approved by the International Mineralogical Association Commission on New Minerals, Nomenclature and Classification (IMA2011-077).

Introduction

The last thermal crisis, which started at Vulcano, Aeolian Islands, Italy in 1988 and reached a maximum in 1993, was characterised by an intense deposition of interesting and rare sublimate minerals. With the aim of investigating the correlation between the deposition of the mineralogical phases and the fumarole temperature, composition of the gas phase and the volcanic activity, our team began a systematic mineralogical investigation, which since 1994, has led to the discovery of a large variety of rare phases and new minerals (Garavelli, 1994; Garavelli and Vurro, 1994; Ferrara *et al.*, 1995; Coradossi *et al.*, 1996; Borodaev *et al.*, 1998, 2000, 2001, 2003; Vurro *et al.*, 1999; Cheynet *et al.*, 2000; Garavelli *et al.*, 1997, 2003, 2005, 2013, 2014; Pinto *et al.*, 2006a, 2006b, 2006c, 2008, 2011, 2014, 2015a, 2015b;

Mitolo *et al.*, 2009, 2011, 2013; Balić-Žunić *et al.*, 2016, 2018a, 2018b). The abundance and variety of minerals described for La Fossa crater fumaroles attracted worldwide interest in the mineralogy of the area. Within a few years La Fossa crater became a mineralogical attraction for researchers and collectors. The large number of minerals described for the locality, about 30 of which have been discovered only in the last 20 years, makes La Fossa crater of Vulcano one of the most prolific type localities in the world; and in Italy second only to Vesuvius.

Attracted by this 'mineralogical paradise', the late Italian mineral collector G. Scavo visited the locality in 2005 and returned home with a number of interesting mineralogical samples, subsequently given to us for examination. In these samples, some minute, sharp prismatic crystals directly growing on the surface of a pyroclastic breccia focused our attention and resulted in the recognition of the new mineral thermessaite-(NH₄) described herein.

Thermessaite-(NH₄) is the NH₄ analogue of thermessaite, K₂AlF₃(SO₄) (Demartin *et al.*, 2008; type locality also La Fossa

Fig. 1. Location of La Fossa crater at Vulcano Island, Italy and fumarole F11, the sampling site of thermessaite-(NH$_4$) [retrieved from Google Earth^{TM}].

crater), and is identical to an anthropogenic phase from the burning Anna I coal dump at the Anna mine, near Aachen, North Rhine-Westphalia, Germany (Witzke *et al.*, 2015). The International Mineralogical Association (IMA) Commission on New Minerals, Nomenclature and Classification approved both the new mineral and its name (IMA2011-077, Garavelli *et al.*, 2012). The holotype is deposited in the mineral collections of the Museum "C.L. Garavelli" in the "Dipartimento di Scienze della Terra e Geoambientali", Università degli Studi di Bari "Aldo Moro", Italy, sample number 15/nm-V28.

Occurrence and physical properties

Thermessaite-(NH$_4$) is a volcanic sublimate found on the surface of an altered sample of pyroclastic breccia collected in 2005 in close proximity to the active, medium- to high-temperature fumarole F11 ($T \approx 250$–300°C at the time of sampling), located at the rim of La Fossa crater at Vulcano, Aeolian islands, Italy (Fig. 1). Geological and metallogenic data for La Fossa crater area are given in previous papers (Garavelli *et al.*, 1997; Campostrini *et al.*, 2011; Balić-Žunić *et al.*, 2016, and references therein).

Individual single crystals of thermessaite-(NH$_4$) are very rare. Generally the mineral occurs as aggregates of radiating elongated needles in which the individual maximum crystal dimensions are always <0.2 mm. The vitreous crust on which the thermessaite-(NH$_4$) crystals are directly grown, consists of amorphous silica and aluminium silicon fluorides. Sulfur, thermessaite [K$_2$AlF$_3$(SO$_4$)], arcanite [K$_2$(SO$_4$)], mascagnite [(NH$_4$)$_2$(SO$_4$)], and intermediate members of the arcanite–mascagnite series have been identified in the sample rock in which thermessaite-(NH$_4$) was found.

Thermessaite-(NH$_4$) is colourless to white in colour, with a white streak and a vitreous lustre. The minute acicular crystals are transparent to translucent. No twinning was observed. Thermessaite-(NH$_4$) is brittle and no cleavage, parting, or fracture were observed.

The very small dimensions, as well as the softness and friability of the crystals, precluded direct measurements of the refractive indices and physical properties such us density and micro-hardness. The

Table 1. SEM-EDS chemical-analytical data for thermessaite-(NH$_4$) (average of eleven point analyses).

Constituent	Wt.%	Range	S.D.
K$_2$O	3.38	2.77–4.02	0.42
Al$_2$O$_3$	25.35	24.67–26.35	0.57
SO$_3$	36.58	35.48–37.86	0.73
F	26.12	24.77–26.65	0.55
(NH$_4$)$_2$O*	22.47	20.83–22.03	0.33
	113.90		
O = F	−11.00		
Total	102.90		

*The ammonium content was deduced for each point analysis from the K content, taking into account the (NH$_4$,K)$_2$AlF$_3$(SO$_4$) stoichiometry (i.e. NH$_4$ + K = 2 atoms pfu).
S.D. = standard deviation.

calculation of the mean refractive index was done using the Gladstone–Dale constants of Mandarino (1976, 1981). Taking into account the empirical formula, the mean refractive index of thermessaite-(NH$_4$) is 1.54. The calculated density from single-crystal X-ray data and the empirical formula is 2.185 g·cm^{-3}.

Chemical data

Quantitative chemical analyses were obtained using an S360 Cambridge Scanning Electron Microscope coupled with an Oxford-Link Ge ISIS Energy Dispersive Spectrometer equipped with a Super Atmosphere Thin Window$^©$, as this allows better detection of light elements. An energy-dispersive spectrometer (EDS) was chosen for quantitative analyses of the tiny crystals instead of a wavelength-dispersive spectrometer (WDS), because it allows analyses at a non-critical working distance (Ruste, 1979; Acquafredda and Paglionico, 2004; Balić-Žunić *et al.*, 2016) and using a lower probe current. The non-critical working distance permits quantitative EDS analyses even directly on crystal surfaces that are not totally flat, i.e. when it lacks the necessary focusing WDS geometry. Moreover, the minute crystals of thermessaite-(NH$_4$) quickly decompose at a probe current exceeding 3 nA, which generates few X-ray photons only easily detectable by an EDS detector.

The subsample investigated, which consisted of an aggregate of radiating crystals 100 μm in size, was sputtered with a 30 nm-thick carbon film to perform SEM-EDS observations and microanalysis. Operating conditions of the SEM were: 15 kV accelerating voltage, 500 pA probe current, 2500 cps as average count rate on the whole spectrum and typical counting time 100 s. X-ray intensities were converted to wt.% by the ZAF–4/FLS quantitative analysis software support of Oxford-Link Analytical (UK) that allows matching of the peaks of the standards with those of the analysed mineral, but also taking into account the relative contribution of the matrix and when there are partial or complete overlaps among peaks of different elements. The standards employed were: orthoclase (K), corundum (Al), barite (S) and synthetic LiF (F). The analytical results (mean of 11 analyses) are reported in Table 1. The empirical chemical formula, calculated on the basis of 7 anions per formula unit (pfu), is [(NH$_4$)$_{1.85}$K$_{0.15}$]$_{\Sigma2.00}$Al$_{1.06}$F$_{2.94}$S$_{0.98}$O$_{3.06}$. The ammonium content was calculated from the K content, taking into account the (NH$_4$,K)$_2$AlF$_3$(SO$_4$) stoichiometry (NH$_4$ + K = 2 pfu). The simplified formula of thermessaite-(NH$_4$) is (NH$_4$)$_2$AlF$_3$(SO$_4$) which ideally requires (NH$_4$)$_2$O 24.10, Al$_2$O$_3$ 23.59, SO$_3$ 37.05, F 26.36, and O = F −11.10 wt.%.

Crystallography

Single-crystal X-ray diffraction data were collected from a selected crystal fragment (0.110 mm × 0.040 mm × 0.035 mm) from the holotype using a Bruker AXS X8 APEX2 CCD automated diffractometer equipped with a kappa-geometry goniometer and graphite-monochromatised MoKα radiation (50 kV and 30 mA operating conditions). A Miracol fibreoptics capillary collimator (0.3 mm diameter) was used to enhance the beam intensity and to reduce beam divergence. Five sets of 19 frames were used for initial unit-cell determination, whereas complete data collection was accomplished by several ϕ and ω scans with a 0.5° frame width, 120 s exposure time per frame, and a crystal-to-detector distance of 40 mm. The collection strategy was optimised by the *Apex* program suite (Bruker, 2003a). Details about data collection and refinement are summarised in Table 2. Data reduction, including intensity integration, correction for Lorentz, polarisation, background effects, and scale variation, was done using the package *SAINT-IRIX* (Bruker, 2003b). A semi-empirical absorption correction (Blessing, 1995) was applied using the *SADABS* program (Sheldrick, 2008). The approximate minimum and maximum X-ray transmission factors were 0.6535 and 0.7461, respectively.

The structure of thermessaite-(NH$_4$) was refined in the space group *Pbcn* using the full-matrix least-squares program *SHELXL–97* (Sheldrick, 2008), starting from the atomic coordinates of thermessaite (Demartin *et al.*, 2008) and by placing N on the K site. All the hydrogen atoms of the ammonium ion showed up clearly in the difference-Fourier map and were included in the final refinement by restraining N–H distances to the value of 1.00(2) Å and using isotropic atomic displacement parameters. The site occupation factor for the ammonium site was refined taking into account the substitution K$^+$ ↔ NH$_4^+$; the obtained occupancy results [NH$_4$ = 0.86(1) and K = 0.14(1)] give the structural formula [(NH$_4$)$_{1.72}$K$_{0.28}$]AlF$_3$(SO$_4$), in good agreement with the results of the chemical analyses (Table 1).

The refinement converged to the agreement R(F) value of 0.0367 for 672 observed reflections [$I > 2\sigma(I)$]. Scattering factors for neutral atoms were taken from the *International Tables for X-ray Crystallography* (Ibers and Hamilton, 1974). In the final refinement anisotropic displacement factors were used for all the atoms with the exception of hydrogens of the ammonium group.

Single-crystal X-ray diffraction data were also obtained from a crystal (0.02 mm × 0.03 mm × 0.12 mm) of the anthropogenic material recovered from the burning Anna I coal dump of the Anna mine, Aaachen, Germany, using a Bruker ApexII diffractometer (equipped with a CCD detector) with MoKα radiation (for details see Table 2). The measured intensity data were processed with the Bruker program suite *APEX2*, including a multi-scan absorption correction with *SADABS* (Sheldrick, 2002). A full-matrix least-squares refinement on F^2 (*SHELXL–97*, Sheldrick, 2008), with scattering factors for neutral atoms, was performed starting from atomic coordinates of thermessaite, leading to a final R(F) of 0.0372, and the structural formula [(NH$_4$)$_{1.70}$K$_{0.30}$]AlF$_3$(SO$_4$), very similar to that of the type material. Although all H atoms of the NH$_4$ group could be located on the difference-Fourier map, their N–H bond lengths had to be restrained as described for the Vulcano sample and their isotropic displacement parameters fixed to 0.08 Å^2, in agreement with the observation that at least two of them seemed to be involved in bifurcated hydrogen bonds.

Fractional atomic coordinates, occupancies, and displacement parameters for the natural thermessaite-(NH$_4$) from Vulcano

Table 2. Summary of parameters describing data collection and refinement for thermessaite-(NH$_4$) and for the anthropogenic phase from Anna mine.

	New mineral from Vulcano	Anthropogenic phase
Crystal data		
Crystal-structural formula	[(NH$_4$)$_{1.72}$K$_{0.28}$]AlF$_3$(SO$_4$)	[(NH$_4$)$_{1.70}$K$_{0.30}$]AlF$_3$(SO$_4$)
Crystal dimensions (mm)	0.035 × 0.040 × 0.110	0.02 × 0.03 × 0.12
Crystal system, space group	Orthorhombic, *Pbcn*	Orthorhombic, *Pbcn*
a (Å)	11.3005(3)	11.289(2)
b (Å)	8.6125(3)	8.598(2)
c (Å)	6.8501(2)	6.851(1)
V (Å^3)	666.69(4)	665.0(2)
Z	4	4
Temperature (K)	293	293
D_x (g/cm^3)	2.224	2.208
Data collection		
X-ray conditions (kV, mA)	50, 30	50, 30
Wavelength of radiation (Å)	0.71073	0.71073
Detector-to-sample distance (mm)	40	35
Number of frames	695	425
Rotation width per frame (°)	0.5	2
Measuring time (s)	120	400
2θ$_{max}$ (°)	61.04 (d = 0.70 Å)	70.56 (d = 0.615 Å)
Independent reflections	959	1478
Reflections with $Fo > 4\sigma$ (Fo)	672	916
R_{int}, R_σ	0.0445, 0.0422	0.0650, 0.0496
Ranges of h, k, l	$-16 \le h \le 13$	$-17 \le h \le 18$
	$-12 \le k \le 11$	$-10 \le k \le 13$
	$-9 \le l \le 7$	$-10 \le l \le 11$
Refinement		
R [$F_o > 4\ \sigma\ (F_o)$]	0.0367	0.0386
R (all data)	0.0685	0.0902
wR [$F_o > 4\ \sigma\ (F_o)$]	0.0752	0.0815
wR (all data)	0.0868	0.0977
Goof	1.028	1.009
Refined parameters	70	67
Weighting scheme a, $b^\star$	0.038	0.041
	0.4443	0.49
Δρ$_{min}$, Δρ$_{max}$ (e^-/Å^3)	−0.39, 0.32	−0.63, 0.38

*w=1/[$\sigma^2(F_o^2)$+$(aP)^2$+bP] where P =[$max(F_o)^2$+2$(Fc)^2$]/3

and the corresponding anthropogenic material from the Anna mine are presented in Table 3, while selected interatomic distances are listed in Table 4. The crystallographic information files with crystal-structure data of both samples, as well as tables of structure factors, have been deposited with the Principal Editor of *Mineralogical Magazine* and are available as Supplementary material (see below). The powder X-ray diffraction pattern calculated from the single-crystal structure model of the holotype is given in Table 5.

Description of the crystal structure

A polyhedral representation of the crystal structure of thermessaite-(NH$_4$) from Vulcano is given in Fig. 2. It consists of chains of corner-sharing AlF$_4$O$_2$ octahedra running along [001] and joined to each other by sharing two fluorine atoms at opposite vertices. The bridging Al–F2 distances are longer than the non-bridging Al–F1 distances (Table 4). Similar features are observed in the structure of thermessaite (Demartin *et al.*, 2008). The two oxygen atoms at the remaining equatorial corners are shared with SO$_4$ tetrahedra (Fig. 2b), which ensure further connection of adjacent AlF$_4$O$_2$ octahedra, so forming ribbons

Table 3. Atomic coordinates, occupancies (s.o.f.) and displacement factors (Å^2) for thermessaite-(NH$_4$) and for the anthropogenic phase from the Anna mine.

Atom	x	y	z	Occupancy	U^{11}	U^{22}	U^{33}	U^{23}	U^{13}	U^{12}	U_{eq}/U_{iso}
Thermessaite-(NH$_4$)											
Al	½	0	0	1	0.0169(4)	0.0128(4)	0.0086(5)	−0.0001(3)	0.0011(4)	−0.0013(4)	0.0128(2)
F1	0.8493(1)	0.4539(2)	0.4779(2)	1	0.0176(6)	0.0238(7)	0.0232(9)	−0.0024(6)	−0.0020(6)	−0.0036(5)	0.0216(3)
F2	½	0.0779(2)	¼	1	0.029(1)	0.0154(9)	0.0099(9)	0	0.0015(8)	0	0.0182(4)
S	0	0.19620(8)	¼	1	0.0218(4)	0.0115(3)	0.0133(4)	0	0.0007(3)	0	0.0155(2)
O1	−0.0972(2)	0.1039(2)	0.3242(3)	1	0.036(1)	0.0248(9)	0.026(1)	0.0055(8)	0.0026(8)	−0.0135(8)	0.0290(4)
O2	−0.0471(2)	0.2985(2)	0.0914(2)	1	0.0261(8)	0.0150(7)	0.014(1)	0.0024(7)	−0.0046(7)	−0.0025(6)	0.0185(4)
N	0.6939(2)	0.3206(2)	0.2079(3)	0.86(1)	0.0311(9)	0.0307(9)	0.036(1)	−0.009(8)	−0.007(8)	0.0021(7)	0.0327(4)
K	0.6939(2)	0.3206(2)	0.2079(3)	0.14(1)	0.0311(9)	0.0307(9)	0.036(1)	−0.009(8)	−0.007(8)	0.0021(7)	0.0327(4)
H1	0.667(6)	0.357(8)	0.078(5)	0.86(1)							0.16(3)
H2	0.755(5)	0.379(7)	0.28(1)	0.86(1)							0.17(3)
H3	0.693(5)	0.208(2)	0.197(9)	0.86(1)							0.11(2)
H4	0.637(5)	0.329(8)	0.314(8)	0.86(1)							0.15(3)
Anthropogenic phase											
Al	½	0	0	1	0.0171(3)	0.0147(4)	0.0089(3)	−0.0001(3)	0.0007(3)	−0.0010(3)	0.0136(2)
F1	0.84925(10)	0.45388(13)	0.47814(17)	1	0.0195(6)	0.0257(6)	0.0218(6)	−0.0021(5)	−0.0025(5)	−0.0032(5)	0.0223(3)
F2	½	0.07776(17)	¼	1	0.0313(8)	0.0166(7)	0.0094(6)	0	0.0012(7)	0	0.0191(3)
S	0	0.19621(7)	¼	1	0.0220(3)	0.0131(3)	0.0127(3)	0	0.0005(3)	0	0.0159(2)
O1	−0.09724(15)	0.10380(17)	0.3239(2)	1	0.0372(9)	0.0258(8)	0.0271(8)	0.0054(7)	0.0019(7)	−0.0126(7)	0.0300(4)
O2	−0.04722(14)	0.29892(15)	0.09130(19)	1	0.0272(7)	0.0166(7)	0.0150(6)	0.0017(5)	−0.0051(6)	−0.0024(6)	0.0196(3)
N	0.69395(14)	0.32039(17)	0.2072(2)	0.845(4)	0.0341(9)	0.0334(9)	0.0316(9)	−0.0089(6)	−0.0067(6)	0.0012(6)	0.0334(6)
K	0.69395(14)	0.32039(17)	0.2072(2)	0.155(4)	0.0341(9)	0.0334(9)	0.0316(9)	−0.0089(6)	−0.0067(6)	0.0012(6)	0.0334(6)
H1	0.670(4)	0.348(5)	0.073(4)	0.848							0.08
H2	0.764(3)	0.375(4)	0.252(6)	0.848							0.08
H3	0.700(4)	0.214(3)	0.165(6)	0.848							0.08
H4	0.643(3)	0.318(4)	0.322(5)	0.848							0.08

Table 4. Selected interatomic distances (Å) for thermessaite-(NH$_4$) and the anthropogenic phase from the Anna mine.

	Holotype	Anthropogenic phase
Al–F1	1.756(1) ×2	1.754(1) ×2
Al–F2	1.839(1) ×2	1.839(1) ×2
Al–O2	1.920(1) ×2	1.914(1) ×2
⟨Al–F/O⟩	1.838	1.836
S–O1	1.448(2) ×2	1.447(2) ×2
S–O2	1.497(2) ×2	1.499(1) ×2
⟨S–O⟩	1.473	1.473
N–H1*	0.99(2)	0.97(2)
N–H2	0.98(2)	0.97(2)
N–H3	0.97(2)	0.99(2)
N–H4	0.98(2)	0.97(2)
N···O1	2.789(2)	2.787(2)
N···F1	2.796(2)	2.7992(19)
N···F1'	2.883(2)	2.8744(19)
N···O1'	2.920(3)	2.918(2)
N···F2	3.042(2)	3.0384(19)
N···O2	3.039(2)	3.034(2)
N···F1''	3.055(2)	3.050(2)
N···O1'	3.113(3)	3.109(2)
N···O2'	3.272(3)	3.274(2)

* N–H bond lengths were restrained to 1.00(2) Å (see text).

that extend indefinitely along [001]. The S–O distances are longer for bridging oxygens than for non-bridging oxygen atoms (Table 4). Isolated NH$_4^+$ ions occur in layers parallel to (100) which alternate regularly with (100) layers containing ribbons of corner-sharing AlF$_4$O$_2$ octahedra and associated SO$_4$ groups. The general scheme of the structure as well as bond-distances within the AlF$_4$O$_2$ octahedra and the sulfate groups are very similar to those in thermessaite (Demartin *et al.*, 2008). NH$_4^+$ ions represent significantly distorted tetrahedra with N–H bond

lengths ranging from 0.97(2) to 0.99(2) Å in the structure of the holotype sample from Vulcano. In both the holotype and the Anna mine samples, the NH$_4^+$ ions are partially replaced by K$^+$ ions. Interestingly, but probably a simple coincidence, the refined N:K ratios are very similar [0.86(1):0.14 *vs.* 0.85(4): 0.155]. The NH$_4^+$/K$^+$ ions are located in nine-coordinate sites where they are bonded to five oxygen atoms (O1 and O2) and four fluorine atoms (F1, F2) and thereby provide an important linkage between the chains. The donor–acceptor distances N···O/F range between 2.789(2) and 3.272(3) Å (type material; values for the Anna mine crystal are very similar; Table 4) and reflect weak to very weak hydrogen bonding. The local orientation of the NH$_4^+$ ions in these nine-coordinate sites will be controlled by the significant hydrogen bonding present and probably also indirectly by the (NH$_4$):K ratio.

Genetic features

Thermessaite-(NH$_4$) is a new anhydrous fluoride sulfate from a medium- to high-temperature fumarole at La Fossa volcano crater. Its discovery is a remarkable event, not just because of the simultaneous presence in it of ammonium, aluminium and fluorine as essential constituents, which occurs only in thermessaite-(NH$_4$), but because it also permits us to discuss once more the conditions of mineral deposition at La Fossa crater fumaroles.

Aluminium phases, mainly hydrous sulfates (i.e. alunogen and alunite, etc.) and/or fluorides (i.e. hydrokenoralstonite), are relatively common among volcanic fumarole minerals and their occurrence is generally interpreted as a secondary deposition during the final stage of the process of interaction between volcanic fumarole fluids and wall rocks crossed by the fluids rising to the surface (fumarole encrustations). The cooling and oxidation of high-temperature volcanic gases result in: (1) the formation in proximity of the surface of acidic condensates that react with

Table 5. Calculated X-ray powder diffraction pattern (*d* in Å) for thermessaite-(NH₄) holotype.

I/Iₒ	d(hkl)	h k l	I/Iₒ	d(hkl)	h k l
74	**6.850**	**1 1 0**	1	1.945	4 2 2
100	**5.650**	**2 0 0**	1	1.930	2 4 1
89	**4.844**	**1 1 1**	3	1.921	5 2 1
3	3.889	2 1 1	2	1.904	3 1 3
6	3.646	0 2 1	11	1.900	2 2 3
6	3.451	3 1 0	1	1.886	5 0 2
4	3.425	0 0 2	6	1.883	6 0 0
47	**3.082**	**3 1 1**	1	1.843	5 1 2
56	**3.063**	**1 1 2**	5	1.823	0 4 2
53	**3.063**	**2 2 1**	1	1.803	3 4 1
5	2.825	4 0 0	1	1.778	3 2 3
26	**2.782**	**1 3 0**	2	1.777	6 1 1
1	2.773	2 1 2	6	1.776	5 3 0
28	**2.681**	**0 2 2**	1	1.765	1 3 3
2	2.620	3 2 1	2	1.736	4 3 2
7	2.608	1 2 2	2	1.735	2 4 2
3	2.578	1 3 1	1	1.726	6 2 0
1	2.534	3 0 2	5	1.719	5 3 1
9	2.499	4 1 1	4	1.713	0 0 4
4	2.431	3 1 2	1	1.713	4 4 0
15	2.398	2 3 1	1	1.703	1 5 0
3	2.362	4 2 0	4	1.661	1 1 4
1	2.283	3 3 0	1	1.642	4 2 3
1	2.233	4 2 1	1	1.641	3 4 2
5	2.186	5 1 0	1	1.639	2 0 4
2	2.184	3 2 2	1	1.615	3 3 3
4	2.179	4 0 2	1	1.610	2 1 4
1	2.166	1 1 3	1	1.602	2 5 1
17	2.166	3 3 1	1	1.591	0 2 4
1	2.160	1 3 2	4	1.587	7 1 0
5	2.113	4 1 2	1	1.559	3 0 4
2	2.083	5 1 1	1	1.546	7 1 1
1	2.056	2 1 3	8	1.541	6 2 2
3	2.054	0 4 1	1	1.532	2 2 4
1	2.050	2 3 2	1	1.527	3 5 1
5	2.021	1 4 1	8	1.525	1 5 2
5	2.017	0 2 3	1	1.510	4 3 3
1	2.012	2 4 0	3	1.510	2 4 3
7	1.986	1 2 3			

The strongest lines are given in bold.

Fig. 2. (a) The crystal structure of thermessaite-(NH₄) in a view along the *c* axis. The unit cell is outlined and N–H bonds are shown. (b) The crystal structure of thermessaite-(NH₄) in a view along the [110] axis, perpendicular to the octahedral–tetrahedral chains. Legend: yellow = AlO₄F₂ octahedra, red = SO₄ tetrahedra, blue spheres = N atoms, grey spheres = H atoms, red spheres= O atoms and green spheres = F atoms.

the wall rocks; (2) a differential leaching from the rocks of the elements, according to their different mobility; (3) the precipitation of secondary minerals. Unlike these phases, thermessaite-(NH₄) cannot be considered a secondary mineral, but a primary phase formed by direct deposition from the fumarole steam moving through the rocks to the surface (volcanic sublimate). This is confirmed, not only by the temperature values measured at fumaroles where the new mineral was collected, which prevent the existence of a condensed aqueous phase reacting with the rocks, but also by the morphology and the condition of growth of the mineral. As a matter of fact, thermessaite-(NH₄) appears directly growing from the rocks, sometimes covered by crusts of vitreous amorphous silica and ammonium silico-fluorides, in small radiating aggregates of acicular and elongated individual crystals, with no signs of dissolution and recrystallisation.

Ammonium mineral phases are relatively abundant among sublimate minerals from La Fossa crater fumaroles, and their occurrence is due to the relatively high ammonia content in the volcanic fluids discharging from the area. Ammonium minerals generally occur around vents with medium–high temperature values (300–200°C) and generally consist of chlorides (containing traces of Br and I) (i.e. salammoniac) and complex chloride–
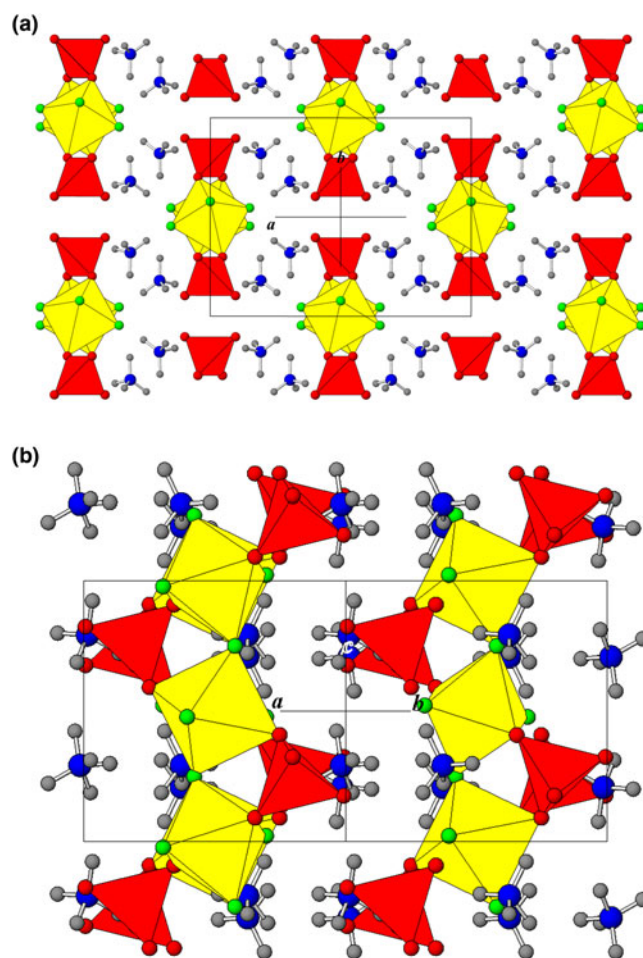
sulfates and sulfates. This assemblage is indicative of a chlorine-rich environment, in which the elements known to form volatile metal chlorides (Me = Na, Pb, Bi, Sn and Fe) can be transported easily in the fumarolic steam as MeClₓ complexes. The chlorine complexes act as carriers for the metals and, in the generally reducing, H₂S-rich conditions observed at Vulcano fumaroles at the end of last century, form sulfochloride complexes which act as catalysts for the reactions leading to the formation of the high-temperature sulfide and sulfosalt assemblage (Balić-Žunić *et al.*, 2016, and references therein). In that context, the anoxic conditions of the environment and the existing fumarole gas composition at that time prevented the formation of high-temperature metal sulfates, which are generally abundant in high-temperature fumarole environments in other volcanoes around the world.

Since the beginning of the 2000s, the thermodynamic conditions at fumaroles at La Fossa crater of Vulcano have gradually changed. Temperature values remained high, but the percentage of deposited sulfides and sulfosalts was gradually reduced, new phases began to form, and were subsequently described as new minerals. They consist mainly of metal chlorides, complex chloride–sulfates and sulfates, the occurrence of which is indicative of
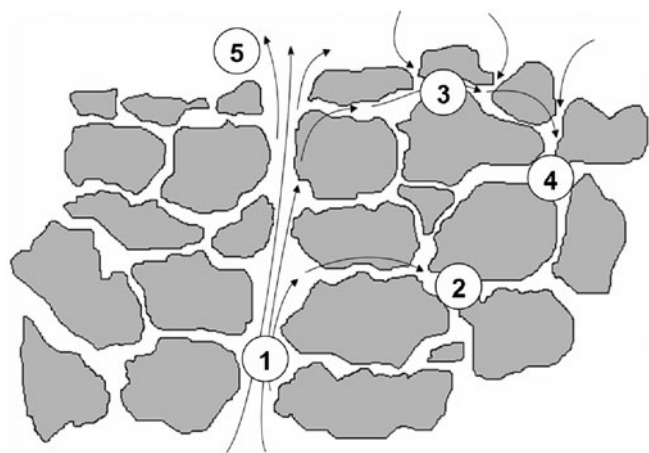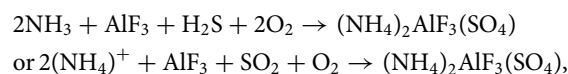
Fig. 3. Scheme of the processes occurring in medium- to high-temperature fumaroles of La Fossa crater: (1) volcanic gases rise to the surface interacting with wall rocks and leaching selected elements (Si and Al); (2) deposition of high-temperature sublimates in reducing conditions (no interaction with the atmosphere); (3) dilution of volcanic gases with the atmosphere and deposition of phases (halides to sulfates) in oxidising conditions (medium–high temperature zone); (4) condensation of the fumarole steam far from the vent and deposition of fumarolic encrustations (hydrous sulfates), in oxidising conditions at ∼100°C or less, after the mixing of the volcanic fluid phase with the atmospheric fluids entering the system, and interaction with the rocks; (5) deposition of medium–high temperature sublimates in reducing conditions. The high fluxes of the gases prevented the incorporation of atmospheric oxygen in the system and the formation of oxidising conditions. High-temperature values at the vent are also due to the high fluxes of gases.

increased oxidising conditions than previously, probably favoured by a reduction of the gas fluxes connected to the volcanic activity, and the consequent increased mixing of the volcanic fumarole steam with the atmosphere in proximity of the surface (Fig. 3). This order of deposition is also consistent with finding the Bi-sulfates leguernite and balićžunićite at Vulcano fumaroles (Garavelli et al., 2014; Pinto et al., 2014, 2015a, b), as well as with the remarkable formation of the complex chloride–sulfates, which could represent the intermediate stage of the transition from a halide to sulfate assemblage after the intrusion of atmospheric oxygen into the system.

The simple ammonium chloride salammoniac, which is very abundant around La Fossa crater fumaroles with temperature values up to 300°C, as well as the new ammonium tin, ammonium lead, and ammonium bismuth chlorides: panichiite (Demartin et al., 2009a), brontesite (Demartin et al., 2009b) and argesite (Demartin et al., 2012), respectively, could be interpreted as the last stage of the transition from a halide to sulfate assemblage in a chlorine-rich environment.

Regardless of the abundance of simple or complex chlorides among La Fossa crater sublimates, minerals containing fluorine are relatively rare here and their finding is always a noteworthy event connected to local increase of the F/Cl ratio in the fumarolic steam. Although fluorides have been reported in many studies of volcanic encrustations (Jacobsen et al., 2014, and references therein, Balić-Žunić et al., 2016, 2018a), the geochemistry and mineralogy of fluorine in the fumarolic environment is poorly known. Fumarole emanations are enriched especially in fluorine because of the condensation of HF gas. As HF reacts strongly with rock-forming silicates, its role in the alteration of rocks crossed by volcanic gases rising to the surface is important (Africano and Bernard, 2000 and references therein). The

leaching of the rocks by HF enriches the volcanic fluids by supplying them with complexes such as SiF_4, BF_3, or AlF_3, which reach the surface and contribute to the sublimate deposition around, and in, the inner areas of fumaroles. At Vulcano, BF_4^- ions participate in the formation of the sublimate barberiite, NH_4BF_4, and SiF_6^- ions determine the formation of Na and K silicofluoride minerals such as malladrite, hieratite and demartinite. However, to the best of our knowledge, the ammonium silicofluorides cryptohalite and bararite [both $(NH_4)SiF_6$] have never been found there. Nevertheless, the thin crust of vitreous and amorphous ammonium silicofluorides covering the rocks of the fumarole in which thermessaite-(NH_4) was found, simultaneously prove the existence of ammonium silicofluorides in Vulcano fumaroles and increase the potential for finding cryptohalite and bararite among sublimates from the area. In this context, thermessaite-(NH_4) represents a very interesting find at Vulcano, to this day second only to barberiite, containing both ammonium and fluorine as essential constituents. In addition, thermessaite-(NH_4) represents the first ammonium sublimate of Vulcano in which Al is one of the major species-forming elements, presumably formed at Vulcano due to the presence of AlF_3 complexes in the fumarole steam. The transport of aluminium in volcanic emissions in the form of fluoride complexes is commonly reported in the literature, and the finding of the new mineral oskarssonite, AlF_3, among volcanic sublimates from Mt. Hekla, Iceland (Jakobsen et al., 2014) even more confirms the presence of this compound in fumarole environments. Oskarsson (1981) and Rosenberg (1988) suggested that AlF_3 is one of the principal high-temperature volcanogenic salts that form incrustations by fractional condensation of volcanic gases. Its presence in the volcanic steam is due to the leaching of the rocks by HF contained in volcanic steams, according to the reaction $Al_2O_3 + 6HF \rightarrow 2AlF_3 + 3H_2O$. Silicates of the affected rocks are also involved in the reactions, and the equilibrium $SiO_2 + 4HF \rightarrow SiF_4 + 2H_2O$ shifts progressively to the right, with SiF_4 becoming a significant F-bearing molecular species below 300°C (Rosenberg, 1992). The finding of vitreous ammonium-silicofluoride crusts associated with thermessaite-(NH_4) strengthens the hypothesis of the simultaneous leaching from the rocks as the source of Si and Al in fumarole fluids at Vulcano, and provides further clues to the transport of both these elements as fluorine complexes. Laboratory investigations in the system AlF_3–Al_2O_3–H_2O–HF allowed the synthesis of AlF_3 as one of the phases at 450–700°C and demonstrated that, in this system, the AlF_3 hydration grade increases with increasing temperature (Rosenberg, 2006). Thermochemical calculations applied to the cooling of volcanic gases discharging from Mount St. Augustine volcano fumaroles in Alaska (Getahun et al., 1996) indicated that solid AlF_3 starts forming as sublimate at ∼300°C, which is about the same value as measured in the fumarole from which thermessaite-(NH_4) was collected. It could be speculated that at Vulcano the presence of ammonium in the volcanic steam somehow prevented the formation of oskarssonite, AlF_3, favouring the thermessaite-(NH_4) deposition. As in the case of the aforementioned AlF_3 laboratory experiments (Rosenberg, 2006), the absence of hydration in thermessaite-(NH_4) could be interpreted as due to deposition at relatively low temperature. A possible reaction explaining the condensation of the new mineral is the following:

$$2NH_3 + AlF_3 + H_2S + 2O_2 \rightarrow (NH_4)_2AlF_3(SO_4)$$
$$\text{or } 2(NH_4)^+ + AlF_3 + SO_2 + O_2 \rightarrow (NH_4)_2AlF_3(SO_4),$$

which requires the incorporation of oxygen in the system. Similar reactions not involving AlF_3 could lead to the deposition of mascagnite, which has been found associated with thermessaite-(NH_4). Mascagnite deposition presumably follows immediately, or happens simultaneously, to the thermessaite-(NH_4) formation, according to the following reaction:

$$2NH_3 + H_2S + 2O_2 \rightarrow (NH_4)_2(SO_4)$$
$$\text{or } 2(NH_4)^+ + SO_2 + O_2 \rightarrow (NH_4)_2(SO_4).$$
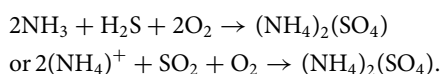
This mineralogical assemblage represents a remarkable intermediate stage of the transition from halide to sulfate in a fluorine-rich, oxidised environment, and the thermessaite-(NH_4) formation is interpreted as the end stage of the fluoride/sulfate conversion. Possible processes explaining the mineralogy observed are shown schematically in Fig. 3. The high-temperature volcanic gases interact with the wall rocks and cool during their uprising through the fumarole vent. Due to the lowering of the flow rate and the pronounced fracturing of the near-surface rocks, atmospheric O_2 enters into the fumarole vent leading to the oxidation of the gas phase. The presence of native sulphur in the mineral assemblage is also consistent with this process as it can be produced by the reaction $SO_2 + 2H_2S \rightarrow 3S + 2H_2O$ (Mizutani and Sugiura, 1996).

The finding of thermessaite-(NH_4) in the burning Anna I dump of the Anna coal mine in Aldsdorf, Germany, although remarkable, it is not surprising due to: (1) the similarity of the burning-coal steams with volcanic exhalations (the vent which yielded the anthropogenic thermessaite-(NH_4) samples had a temperature of 170°C); (2) the strong analogies in the mineralogy of La Fossa crater fumaroles and the burning dump at Anna mine (Witzke et al., 2015). Solid condensed phases known both from La Fossa crater and the Anna I mine dump include sulphur, selenium, salammoniac, metal chlorides, (NH_4)-metal-sulfate chlorides, metal-sulfate fluorides, anhydrous and hydrous metal-sulfates. The absence of sulfides and sulfosalts at the Anna Mine is probably due to the negligible Pb and Bi concentrations in both coal and associated (sedimentary) country rocks. Also the burning dump may feature more oxidising near-surface conditions, which would prevent the deposition of these reduced sulfide and sulfosalt phases and, conversely, favour the high-temperature anhydrous sulfate formation.

In both the mentioned environments, the gas composition and the temperatures at depth are enough to permit the mobilisation of volatile elements by the leaching of selected elements from the rocks crossed by the acidic fluids rising to the surface. At fumaroles, and on the surface of the dump, the processes leading to mineral deposition are the same, except water condensation which is surely more abundant in the dump than in fumaroles, as testified by the abundance of hydrous sulfates at Anna I compared with the Vulcano medium- to high-temperature fumaroles.

References

Acquafredda P. and Paglionico A. (2004) SEM-EDS microanalyses of microphenocrysts of Mediterranean obsidians: a preliminary approach to source discrimination. *European Journal of Mineralogy*, **16**, 419–429.

Africano F. and Bernard A. (2000) Acid alteration in the fumarolic environment of Usu volcano, Hokkaido, Japan. *Journal of Volcanology and Geothermal Research*, **97**, 475–495.

Balić-Žunić T., Garavelli A., Jakobsson S.P., Jonasson K., Katerinopoulos A., Kyriakopoulos K. and Acquafredda P. (2016) Fumarolic minerals: an overview of active European volcanoes. In: *Updates in Volcanology – From Volcano Modelling to Volcano Geology* (Karoly Nemeth Dr., editor). InTech, London. https:doi.org/10.5772/64129. Available from: http://www.intechopen.com/books/updates-in-volcanology-from-volcano-modelling-to-volcano-geology/fumarolic-minerals-an-overview-of-active-european-volcanoes.

Balić-Žunić T., Garavelli A. and Mitolo D. (2018a) Topsøeite, $FeF_3(H_2O)_3$, a new fumarolic mineral from the Hekla volcano, Iceland. *European Journal of Mineralogy*, **30**, 841–848.

Balić-Žunić T., Garavelli A., Pinto D. and Mitolo D. (2018b) Verneite, $Na_2Ca3Al2F14$, a new aluminum fluoride mineral from Icelandic and Vesuvius fumaroles. *Minerals*, **8**, 553, doi: 10.3390/min8120553.

Blessing R.H. (1995) An empirical correction for absorption anisotropy. *Acta Crystallographica*, **A51**, 33–38.

Borodaev Y.S., Garavelli A., Kuzmina O.V., Mozgova N.N., Organova N.I., Trubkin N.V. and Vurro F. (1998) Rare sulfosalts from Vulcano, Aeolian Islands, Italy. I. Se-bearing kirkiite, $Pb_{10}(Bi,As)_6(S,Se)_{19}$. *The Canadian Mineralogist*, **36**, 1105–1114.

Borodaev Y.S., Garavelli A., Garbarino C, Grillo S.M., Mozgova N.N., Organova N.I., Trubkin N.V. and Vurro F. (2000) Rare sulfosalts from Vulcano, Aelian Islands, Italy. III. Wittite and Cannizzarite. *The Canadian Mineralogist*, **38**, 23–34.

Borodaev Y.S., Garavelli A., Garbarino C., Grillo S.M., Mozgova N.N., Uspenskaya T.Y. and Vurro F. (2001) Rare sulfosalts from Vulcano, Aeolian Islands, Italy. IV. Lillianite. *The Canadian Mineralogist*, **39**, 1203–1215.

Borodaev Y.S., Garavelli A., Garbarino C., Grillo S.M., Mozgova N.N., Paar W.H., Topa D. and Vurro F. (2003) Rare sulfosalts from Vulcano, Aeolian Islands, Italy. V. Selenian heyrovskýite. *The Canadian Mineralogist*, **41**, 429–440.

Bruker (2003a) *SAINT-Plus.* Bruker AXS Inc., Madison, Wisconsin, USA.

Bruker (2003b) *SAINT-IRIX*, Bruker AXS Inc., Madison, Wisconsin, USA.

Campostrini I., Demartin, F., Gramaccioli, C.M. and Russo, M. (2011) *Vulcano: tre secoli di mineralogia*. Associazione Micro-mineralogica Italiana, Cremona, Italy [in Italian].

Cheynet B., Dall'aglio M., Garavelli A., Grasso M.F. and Vurro F. (2000) Trace elements from fumaroles at Vulcano Island, Italy: rates of transport and a thermochemical model. *Journal of Volcanology and Geothermal Research*, **95**, 273–283.

Coradossi N., Garavelli A., Salamida M. and Vurro F. (1996) Evolution of Br/Cl ratios in fumarolic salammoniac from Vulcano (Aeolian Islands, Italy). *Bulletin of Volcanology*, **58**, 310–316.

Demartin F., Gramaccioli C.M., Campostrini I. and Orlandi P. (2008) Thermessaite, $K_2[AlF_3|SO_4]$, a new ino-aluminofluoride-sulfate from La Fossa crater, Vulcano, Aeolian Islands, Italy. *The Canadian Mineralogist*, **46**, 693–700.

Demartin F., Campostrini I. and Gramaccioli C.M. (2009a) Panichiite, natural ammonium hexachlorostannate(IV), $(NH_4)_2SnCl_6$, from La Fossa crater, Vulcano, Aeolian Islands, Italy. *The Canadian Mineralogist* **47**, 367–372.

Demartin F., Gramaccioli C.M. and Campostrini I. (2009b) Brontesite, $(NH_4)_3PbCl_5$, a new product of fumarolic activity from La Fossa crater, Vulcano, Aeolian Islands, Italy. *The Canadian Mineralogist*, **47**, 1237–1243.

Demartin F., Campostrini I., Castellano C. and Gramaccioli C.M. (2012) Argesite, $(NH_4)_7Bi_3Cl_{16}$, a new mineral from La Fossa Crater, Vulcano, Aeolian Islands, Italy. A first example of the $[Bi_2Cl_{10}]^{4-}$ anion. *American Mineralogist*, **97**, 1446–1451.

Ferrara G., Garavelli, A., Pinarelli, L. and Vurro F. (1995) Lead isotope composition of the sublimates from the fumaroles of Vulcano (Aeolian Islands, Italy): inferences on the deep fluid circulation. *Bulletin of Volcanology*, **56**, 621–625.

Garavelli A. (1994) *Mineralogia e geochimica di fasi vulcaniche condensate: i sublimati dell'isola di Vulcano tra il 1990 ed il 1993*. PhD dissertation, University of Bari, Italy [in Italian].

Garavelli A. and Vurro F. (1994) Barberiite, NH_4BF_4, a new mineral from Vulcano, Aeolian Islands, Italy. *American Mineralogist*, **79**, 381–384.

Garavelli A., Laviano R. and Vurro F. (1997) Sublimate deposition from hydrothermal fluids at the Fossa crater, Vulcano, Italy. *European Journal of Mineralogy*, **9**, 423–432.

Garavelli A., Pinto D. and Vurro F. (2003) Mineralogy of sublimates and fumarole incrustations at Vulcano Island, Italy. Pp. 89–100 in: *Incontri scientifici Special Issue* (S. Fiore, editor), IMAA-CNR, Italy.

Garavelli A., Mozgov, N.N., Orlandi P., Bonaccorsi E., Pinto D., Moëlo Y. and Borodaev Y. (2005) Rare sulfosalts from Vulcano, Aeolian Islands, Italy. VI. Vurroite, $Pb_{20}Sn_2(Bi,As)_{22}S_{54}Cl_6$, a new mineral species. *The Canadian Mineralogist*, **43**, 703–711.

Garavelli A., Mitolo D. and Pinto D. (2012) Thermessaite-(NH_4), IMA 2011-077. CNMNC Newsletter No. 12, February 2012; page 152; *Mineralogical Magazine*, **76**, 151–155.

Garavelli A., Mitolo D., Pinto D. and Vurro F. (2013) Lucabindiite, $(K,NH_4)As_4O_6(Cl,Br)$, a new fumarole mineral from the "La Fossa" crater at Vulcano, Aeolian Islands, Italy. *American Mineralogist*, **98**, 470–477.

Garavelli A., Pinto D., Mitolo D., Bindi L. (2014) Leguernite, $Bi_{12.67}O_{14}(SO_4)_5$, a new Bi oxysulfate from the fumarole deposit of La Fossa crater, Vulcano, Aeolian Islands, Italy. *Mineralogical Magazine*, **78**, 1629–1645.

Getahun A., Reed M.H. and Symonds R. (1996) Mount St. Augustine volcano fumarole wall rock alteration: Mineralogy, zoning, composition and numerical models of its formation process. *Journal of Volcanology and Geothermal Research*, **71**, 73–107.

Ibers J.A. and Hamilton W.C. (1974) *International Tables for X-ray Crystallography, Volume 4*. The Kynoch Press, Birmingham, UK.

Jacobsen M.J., Balić-Žunić T., Mitolo D., Katerinopoulou A., Garavelli A. and Jakobsson S.P. (2014) Oskarssonite, AlF_3, a new fumarolic mineral from Eldfell volcano, Heimaey, Iceland. *Mineralogical Magazine*, **78**, 215–222.

Mandarino, J.A. (1976) The Gladstone-Dale relationship – Part I: Derivation of new constants. *The Canadian Mineralogist*, **14**, 498–502.

Mandarino J.A. (1981) The Gladstone-Dale relationship. IV. The compatibility index and its application. *The Canadian Mineralogist*, **19**, 441–450.

Mitolo D., Pinto D., Garavelli A., Bindi L. and Vurro F. (2009) The role of the minor substitutions in the crystal structure of natural challacolloite, KPb_2Cl_5, and hephaistosite, $TlPb_2Cl_5$, from Vulcano (Aeolian Archipelago, Italy). *Mineralogy and Petrology*, **96**, 121–128.

Mitolo D., Capitani G.C., Garavelli A. and Pinto D. (2011) Transmission electron microscopy investigation of Ag-free lillianite and heyrovskýite from Vulcano, Aeolian Islands, Italy. *American Mineralogist*, **96**, 288–300.

Mitolo D., Demartin F., Garavelli A., Campostrini I., Pinto D., Gramaccioli C.M., Acquafredda P. and Kolitsch U. (2013) Adranosite-(Fe), $(NH_4)_4NaFe_2(SO_4)_4Cl(OH)_2$, a new ammonium sulfate chloride from La Fossa crater, Vulcano, Aeolian Islands, Italy. *American Mineralogist*, **51**, 57–66.

Mizutani Y. and Sugiura T. (1996) The chemical equilibrium of the $SO_2 + 2H_2S \leftrightarrow 3S + 2H_2O$ reaction in solfataras of the Nasudake Volcano. *Bulletin of the Chemical Society of Japan*, **39**, 2411–2414.

Oskarsson N. (1981) The chemistry of Icelandic lava incrustations and the latest stage of degassing. *Journal of Volcanology and Geothermal Research*, **10**, 93–111.

Pinto D., Balić-Žunić T., Garavelli A., Makovicky E. and Vurro F. (2006a) Comparative crystal-structure study of Ag-free lillianite and galenobismutite from Vulcano, Aeolian Islands, Italy. *The Canadian Mineralogist*, **44**, 159–175.

Pinto D., Balić-Žunić T., Garavelli A., Garbarino C., Makovicky E. and Vurro F. (2006b) First occurrence of close-to-ideal kirkiite at Vulcano (Aeolian Islands, Italy): chemical data and single-crystal X-ray study. *European Journal of Mineralogy*, **18**, 393–401.

Pinto D., Balić-Žunić T., Bonaccorsi E., Borodaev Y.S., Garavelli A., Garbarino C., Makovicky E., Mozgova N.N. and Vurro F. (2006c) Rare sulfosalts from Vulcano, Aeolian Islands, Italy. VII. Cl-bearing galenobismutite. *The Canadian Mineralogist*, **44**, 443–457.

Pinto D., Bonaccorsi E., Balić-Žunić T. and Makovicky E. (2008) The crystal structure of vurroite, $Pb_{20}Sn_2(Bi,As)_{22}S_{54}Cl_6$: OD-character, polytypism, twinning, and modular description. *American Mineralogist*, **93**, 719–727.

Pinto D., Balić-Žunić T., Garavelli A. and Vurro F. (2011) Structure refinement of Ag-free heyrovskýite from Vulcano (Aeolian Islands, Italy). *American Mineralogist*, **96**, 1120–1128.

Pinto D, Garavelli A. and Mitolo D. (2014) Baliczunicite, $Bi_2O(SO_4)_2$, a new fumarole mineral from La Fossa crater, Vulcano, Aeolian Islands, Italy. *Mineralogical Magazine*, **78**, 1043–1055.

Pinto D., Garavelli A. and Balić-Žunić T. (2015a) The crystal structure of baliczunicite, $Bi_2O(SO_4)_2$, a new natural bismuth oxide sulphate. *Mineralogical Magazine*, **79**, 597–611.

Pinto D., Garavelli A. and Bindi L. (2015b) Fluorite-related one-dimensional units in natural bismuth oxysulfates: the crystal structures of $Bi_{14}O_{16}(SO_4)_5$ and $Bi_{30}O_{33}(SO_4)_9(AsO_4)_2$ fluorite related one-dimensional units. *Acta Crystallographica*, **B71**, 514–523.

Rosenberg P.E. (1988) Aluminum fluoride hydrates, volcanogenic salts from Mount Erebus, Antarctica. *American Mineralogist*, **73**, 855–860.

Rosenberg P.E. (1992) The hydroxylation of fluorite under hydrothermal conditions. *The Canadian Mineralogist*, **30**, 457–462.

Rosenberg P.E. (2006) Stability relations of aluminum hydroxy-fluoride hydrate, a ralstonite-like mineral in the system $AlF_3–Al_2O_3–H_2O–HF$. *The Canadian Mineralogist*, **44**, 125–134.

Ruste J. (1979) X-Ray spectrometry. Pp 215–267 in: *Microanalysis and Scanning Electron Microscopy* (F. Maurice, L. Meny and R. Tixier, editors). Summer School St-Martin-d'Hères, France, September 11–16, 1978, Les Editions de Physique, Orsay, France.

Sheldrick G.M. (2002) *SADABS Area-Detector Absorption Correction Program*. Bruker AXS Inc., Madison, Wisconsin, UK.

Sheldrick G.M. (2008) A short history of *SHELX*. *Acta Crystallographica*, **A64**, 112–122.

Vurro F., Garavelli A., Garbarino C., Moëlo Y. and Borodaev Y.S. (1999) Rare sulfosalts from Vulcano, Aeolian Islands, Italy. II. Mozgovaite, $PbBi_4(S,Se)_7$, a new mineral species. *The Canadian Mineralogist*, **37**, 1499–1506.

Witzke T., de Wit F., Kolitsch U. and Blaß G. (2015) Mineralogy of the Burning Anna I Coal Mine Dump, Alsdorf, Germany. Pp. 203–240, in: *Coal and Peat Fires: A Global Perspective, Volume 3: Case Studies – Coal Fires* (G.B. Stracher, A. Prakashand and E.V. Sokol, editors). Elsevier, 786 pp.